

Mitigating the vicious cycle between urban heatwaves and building energy systems in Guangdong–Hong Kong–Macao Greater Bay Area

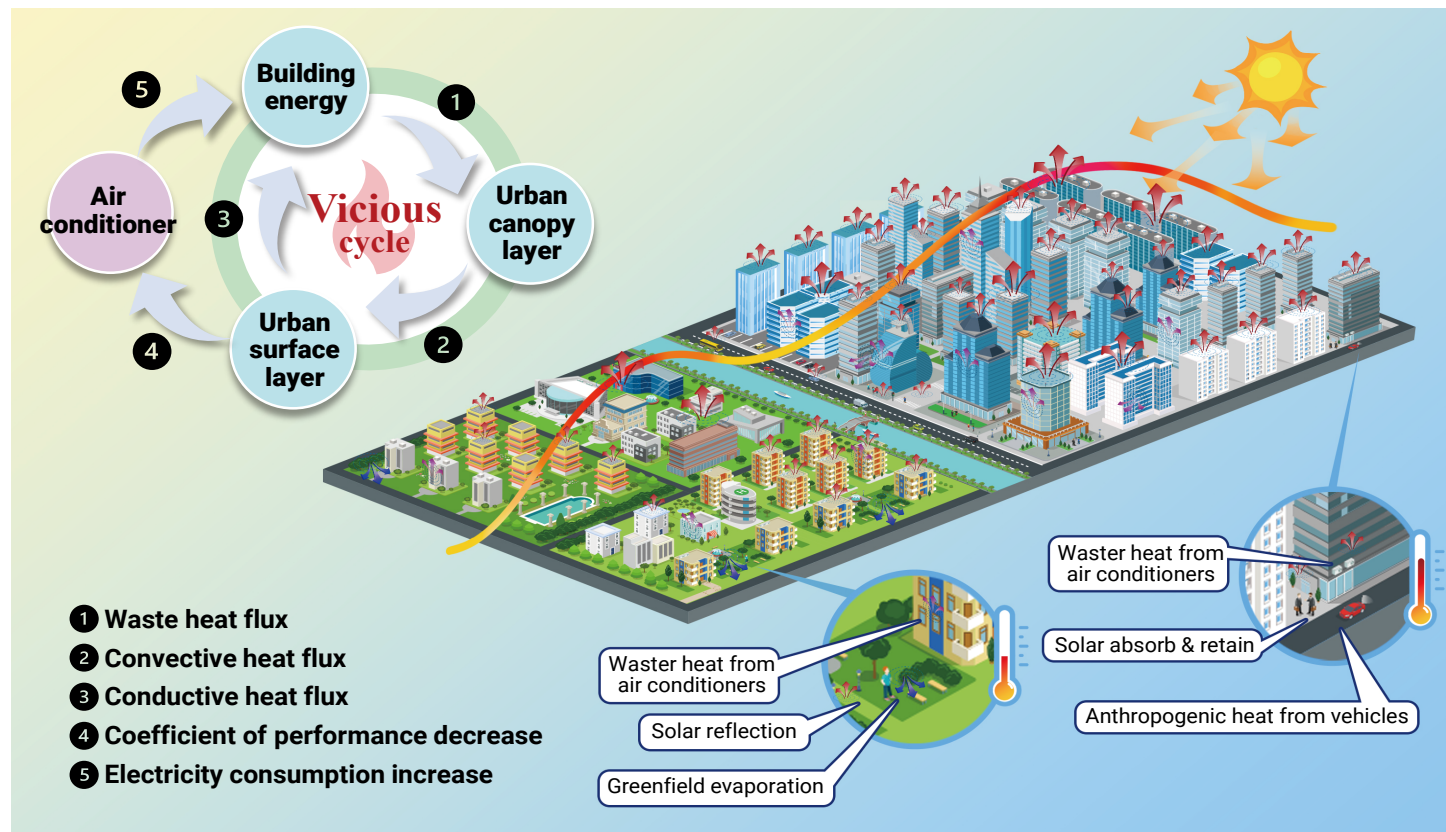
Zhenwei Zhang,^{1,2,3} Hongxun Hui,^{1,2,3,*} and Yonghua Song^{1,2,3}

*Correspondence: hongxunhui@um.edu.mo

Received: October 14, 2024; Accepted: January 13, 2025; <https://doi.org/10.59717/j.xinn-energy.2025.100080>

© 2025 The Author(s). This is an open access article under the CC BY license (<https://creativecommons.org/licenses/by/4.0/>).

GRAPHICAL ABSTRACT



PUBLIC SUMMARY

- The vicious cycle between urban heatwaves and growing cooling demand is already widespread in Guangdong-Hong Kong-Macao Greater Bay Area.
- A joint model coupled with urban microclimate, building energy system, and cooling equipment efficiency are proposed to quantitatively analysis the consequences of vicious cycle.
- A paradigm for addressing vicious cycle from building energy perspective is proposed by rationalizing building pre-cooling and utilizing building virtual storage capabilities.

Mitigating the vicious cycle between urban heatwaves and building energy systems in Guangdong–Hong Kong–Macao Greater Bay Area

Zhenwei Zhang,^{1,2,3} Hongxun Hui,^{1,2,3,*} and Yonghua Song^{1,2,3}

¹State Key Laboratory of Internet of Things for Smart City, University of Macau, Macao, China

²Department of Electrical and Computer Engineering, University of Macau, Macao, China

³University of Macau Advanced Research Institute in Hengqin, Guangdong, China

*Correspondence: hongxunhui@um.edu.mo

Received: October 14, 2024; Accepted: January 13, 2025; <https://doi.org/10.59717/j.xinn-energy.2025.100080>

© 2025 The Author(s). This is an open access article under the CC BY license (<https://creativecommons.org/licenses/by/4.0/>).

Citation: Zhang Z, Hui H, and Song Y. (2025). Mitigating the vicious cycle between urban heatwaves and building energy systems in Guangdong–Hong Kong–Macao Greater Bay Area. *The Innovation Energy* 2:100080.

Urban heatwaves, existing in building neighborhoods, are harsh microclimate phenomena caused by human activities. With global warming and urbanization, exacerbated urban heatwaves are increasing energy-supply burdens and operational risks for building energy systems. At this point, a typical vicious cycle exists among urban microclimate, building energy systems, and cooling equipment, especially in high-density building blocks. Thereby, we propose a joint optimization model to quantify this vicious cycle by combining the urban canopy layer model, urban surface layer model, building energy model, and cooling equipment efficient model. Furthermore, optimal building energy system operation strategies are provided to mitigate the vicious cycle, by utilizing building thermal inertia and arranged building pre-cooling. Case studies are implemented in three typical cities in the Guangdong-Hong Kong-Macao Greater Bay Area in China, including Macao with high population density, Kowloon in Hong Kong with high-rise buildings, and Nanshan in Shenzhen with high-density urban villages. The results demonstrate that the vicious cycle raises urban canopy temperature by 0.97–2.09°C, which correspondingly increases building cooling energy consumption by 1.6–8.4 W/m². By mitigating this vicious cycle based on the proposed optimization model, the energy-saving potential of building blocks can reach 11.2%, 13.4%, and 12.3%, and save 1116.5 MWh, 1724.71 MWh, and 823.23 MWh in the three typical areas, respectively.

INTRODUCTION

In the past few years, numerous countries, such as France, Greece, Italy, Spain, China, et al, have consistently witnessed the breaking of maximum temperature records.^{1,2} Notably, on July 16, 2023, meteorological measurement stations in the Xinjiang region of China recorded an unprecedented temperature of 52.2°C.³ Persistent overheating results in urban heatwaves that continue to erode physical well-being and societal functioning.⁴ To combat urban heatwaves, building sectors have been compelled to turn down operational cooling temperatures and install additional space-cooling equipment. From 1990 to 2016, energy for space cooling is more than tripling, growing faster than for any other end use in buildings.⁵ It is expected that the global average cooling energy needs of residential and commercial buildings will increase by 750% and 275% in 2050, respectively.⁶ With escalating global warming, energy-efficient, sustainable, and regulated operation of cooling systems requires immediate attention.

Recently, extensive research has been carried out in physical modeling, control regulation, and optimal dispatching of cooling systems. The Equivalent Thermal Parameter Model (ETP) is widely employed for describing dynamic heat transfer processes⁷ and establishing the numerical relationship between cooling demand and ambient parameters.⁸ Besides, considering the uncertainties of external weather conditions and indoor anthropogenic heat, model-driven distributional robust optimization⁹ as well as data-driven reinforcement learning approaches¹⁰ are proposed to modify the ETP inputs and outputs. Furthermore, by utilizing the building's thermal inertia and user-adjustable comfort zone, cooling systems achieve virtual energy storage capability, meaning that brief power adjustments cause no effect on cooling demand. This capability supports cooling systems participation in demand response to realize energy-saving,¹¹ renewable energy accommoda-

tion,¹² and peak-valley regulation.¹³ However, most existing research depends heavily on meteorological forecasts or observations from weather stations as external inputs. The reality is that the micro-scale meteorological conditions surrounding buildings play a crucial role in determining the performance of cooling systems. Moreover, most research simplifies the energy conversion process between electricity and cooling based on the fixed coefficient of performance (COP). The reality is that excessively high operating temperatures of condensing units will seriously reduce COP or even stop cooling.

In urban centers, the air temperature of building blocks is generally higher than that in the surrounding rural hinterland, a typical urban microclimate phenomenon known as 'urban heat island (UHI)'.^{14,15} As urbanization advances, urban microclimate is getting more serious and exhibits a strong correlation with urban form, building geometry, land use, and human activities.¹⁶ Over the past decade, the urban heat island effect has become increasingly dramatic with the global urbanization process, resulting from massive anthropogenic heat emissions, less vegetation evaporation, heat absorption, and retention in hard surfaces, wind resistance, and solar radiation reflected by dense tall buildings.^{17–20} In Athens, the mean heat island intensity (HII) exceeds 10°C, but in the very central Athens area, the heat island intensity may reach 15°C.²¹ For now, UHI is further exacerbated by global climate change leading to more frequent and extreme heatwaves, which have been documented in more than 400 major cities around the world.

Excessive urban microscale temperatures contribute directly to the energy consumption of the cooling system. The cooling electricity demand and average cooling penalty induced by UHI markedly increased by up to 40%²² and 2.3 kWh/m²/y/°C,²³ respectively. Regrettably, not only is the cooling demand in urban areas constantly rising due to the exacerbation of UHI but there is also substantial evidence indicating that the anthropogenic waste heat generated by air conditioners (ACs) has emerged as a significant contributor to the intensification of UHI.^{24,25} During a heat wave, air conditioners from urban buildings can add 20% of heat to the outside air, compared to regular summer weather.²⁶ In some typical cities, the waste heat emitted by air conditioners has increased the UHI intensity by more than 2°C.²⁷ In Phoenix, United States, and Madrid, Spain, the 2m temperature rises by 1.75°C²⁸ and 1.5°C to 2°C,²⁹ respectively. In Wuhan, China, the outdoor air temperature has quantitatively been determined to rise by 2.5°C as a result of using air conditioners.³⁰ Hence, there has been a clear vicious cycle between urban microclimate and building cooling demand, where rising ambient temperatures cause cooling equipment to overload, and the resulting waste heat further exacerbates the UHI around the building. With global warming and urbanization, quantifying and mitigating the above vicious cycle will become the key issue for building energy-saving and urban environmental governance.

Relying on meteorological tools and historical statistics, the relationship between cooling energy consumption and microclimate conditions can be quantitatively described and the existence of the vicious cycle described above can be further verified. A numerical simulation system³¹ is proposed to evaluate the impact of anthropogenic heat fluxes on urban boundary layer climate. However, satellite and weather station measurements tend to underestimate the real temperature around buildings. Moreover, meteorological simulations have large spatial scales and cannot reveal the detailed

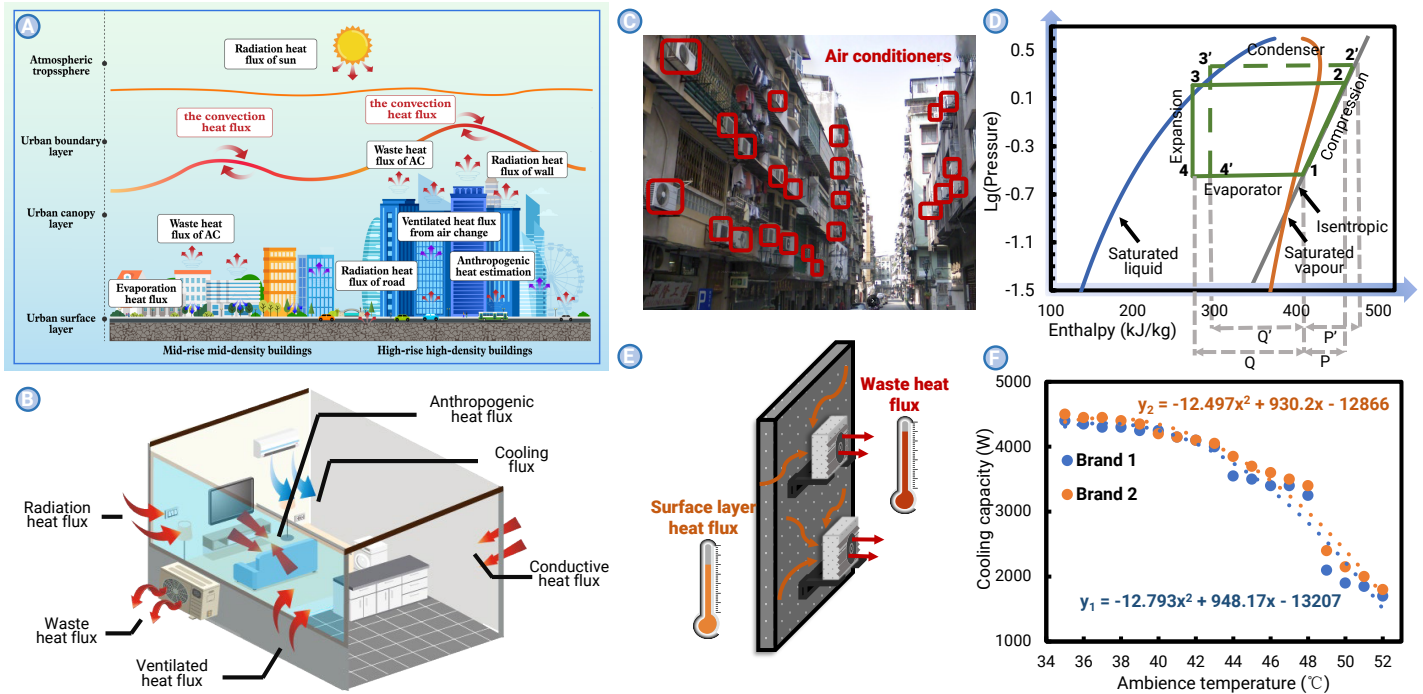


Figure 1. The joint model framework consists of urban microclimate model & building energy system model, and the interaction between microclimate and cooling equipment.

processes of microclimate interactions with buildings in the neighborhood. Urban canopy parameterizations are first taken into account inside a mesoscale meteorological model, coupling a one-dimensional urban canopy model and building energy model.³² Meanwhile, it has further been extended to analyze the feedback mechanism on how the waste heat affects the heat balance in the urban canopy layer.³³ Bueno et al,³⁴ consider that operational weather stations are usually located in open areas, without nearby obstructions, and outside the city. They propose an urban weather generator to calculate urban air temperatures using meteorological information measured at an operational weather station.³⁵ The above-mentioned studies provide numerical analysis closer to reality for microclimate simulation and building energy consumption prediction in urban neighborhoods. However, mitigating the vicious cycle that occurs between microclimate and cooling systems remains a key challenge. Some researchers have suggested increasing vegetation area and spreading out buildings to mitigate UHI,³⁶⁻³⁸ which is inappropriate for urban centers with dense building clusters and would be costly to retrofit old urban areas.

Based on the above analysis, there is an obvious vicious cycle between urban microclimate and building energy systems, especially in high-density building blocks. Refined modeling methods and optimal operation strategies are urgently needed to mitigate this vicious cycle. The major contributions of this paper are threefold:

(1) A refined thermal model integrating the urban canopy layer model, urban surface layer model, building energy model, and cooling equipment efficiency model is proposed to quantitatively calculate the vicious cycle between urban microclimate and building energy system. The building's surrounding temperature distribution and dynamic energy demand can be efficiently calculated.

(2) To mitigate the vicious cycle, a joint optimization strategy is proposed considering the building's thermal inertia and user-adjustable comfort zone. By pre-cooling before urban temperature rises and COP drops, it can effectively avoid large amounts of waste heat emissions in periods of severe vicious cycles.

(3) The typical cities in the Greater Bay Area that experience high temperatures are selected to validate the proposed interactive model. Realistic simulation cases are built based on weather station data, building data, GIS, and historical energy consumption data. The proposed optimization strategies are demonstrated to be effective in mitigating urban heatwaves and reducing

energy consumption in multiple building blocks.

METHODS

Urban microclimate model

To establish the numerical relationship between the building energy system and the surrounding microclimate conditions, we applied a validated urban thermal model,³³⁻³⁶ consisting of urban boundary layer model, urban canopy layer model, and urban surface layer model as shown in Figure 1A. The data of the urban boundary layer is from geostationary operational environmental satellite (data from National Weather Science Data Centre³⁹), which is the initial condition and upper boundary of the canopy layer.

The urban canopy layer, which is the area above ground level up to 1.5 times the height of the building, directly interacts with the building energy system.^{33,34} In microscale meteorological models (below 1km in diameter), the temperature distribution in the urban canopy layer is influenced by the type of underlying surface, which affects the transfer and accumulation of heat flux around the building. To simulate the approximate microclimate conditions of buildings at different locations, we horizontally divide the urban canopy into different building blocks based on the density, height, and type of buildings (data from the Institute of Geographic Sciences and Natural Resources Research, CAS⁴⁰) and the green space distribution (data from OpenStreetMap⁴¹). For each building block, the urban canopy layer absorbs and accumulates both natural and anthropogenic heat sources, and transfers heat flux with the urban boundary layer and surface layer, described as:

$$\rho c_p V_{R,uc} \frac{d\theta_{R,uc}}{dt} = \rho c_p q_{R,ubl} (\theta_{ubl} - \theta_{R,uc}) + Q_{R,waste} + \sum_{k \in \psi_{R,k}} \rho c_p q_{k,is} (\theta_{k,is} - \theta_{R,uc}) + E_{R,an} A_{R,u} + h_{R,co} (A_{R,w} + A_{R,u}) (\theta_{R,sur} - \theta_{R,uc}), \quad \forall k \in \psi_{R,k}, R \in \psi_r \quad (1)$$

where $\theta_{R,uc}$ and $\theta_{R,sur}$ are the temperature of urban canopy layer and surface layer in block R , respectively; θ_{ubl} is the temperature of urban boundary layer; $\theta_{k,is}$ is the indoor temperature of building k ; ρ and c_p are the density and specific heat capacity of air, respectively; $V_{R,uc}$ is the control volume of urban canopy layer; $A_{R,u}$ is the plan area of urban canopy layer in block R , including the sum of the areas of roof surfaces $A_{R,r}$, artificial ground surfaces $A_{R,a}$, and vegetated surfaces $A_{R,v}$; $A_{R,w}$ is the total area of wall in block R ; $q_{R,ubl}$ is the

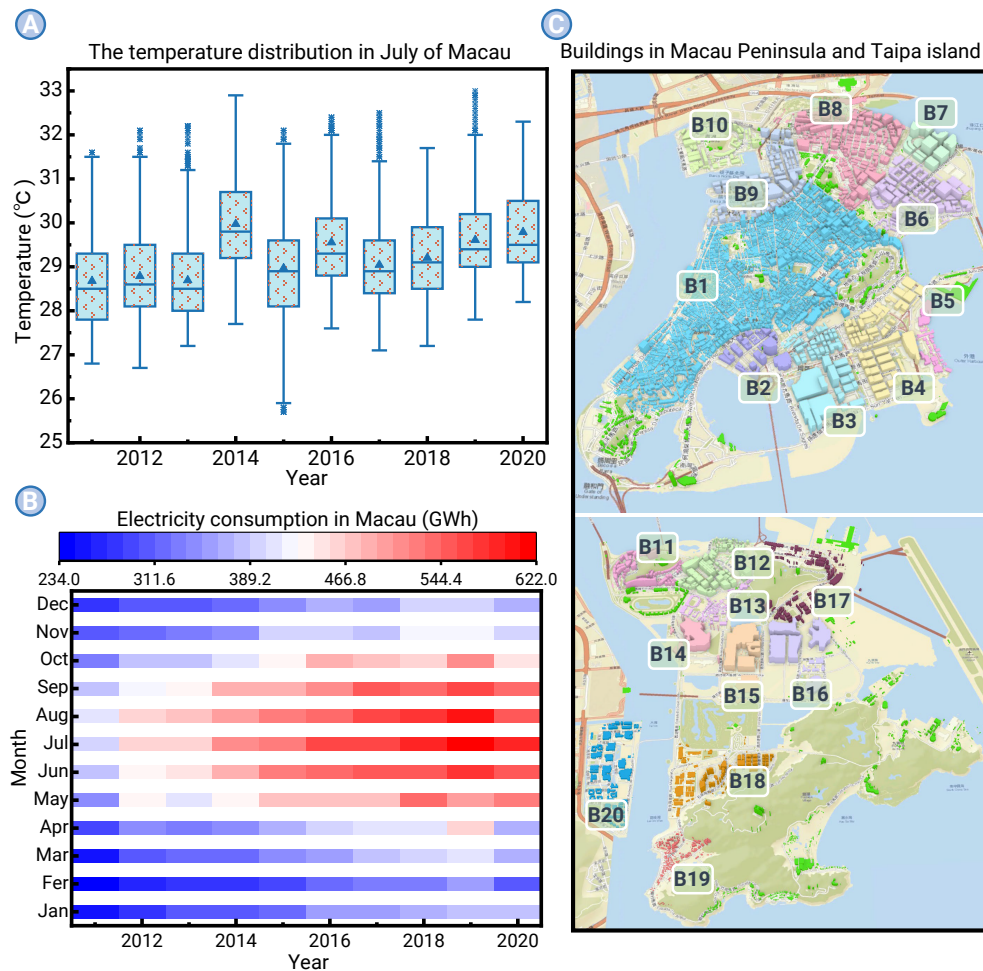


Figure 2. Climate change, energy consumption and building characteristics of Macao.

between the upper surface and the depth having a constant temperature. For each building block, solar radiation is the primary heat source in the urban surface layer. However, due to the heat storage properties of artificial surfaces, the wind resistance of high-density buildings, and the lack of green spaces, the accumulated heat in the urban surface layer cannot be effectively diffused, resulting in a continuous temperature rise. The heat transfer process among the urban surface layer, the urban canopy, and buildings is described in (6):

$$\sum \rho_i c_i \Delta x_{R,i} A_{R,i} \frac{d\theta_{R,sur}}{dt} = (1 - \beta_R) I_R A_{R,u} + k_{R,v} A_{R,v} \frac{\theta_{R,wx,v} - \theta_{R,sur}}{\Delta x_{R,v}} + k_{R,a} A_{R,a} \frac{\theta_{R,wx,a} - \theta_{R,sur}}{\Delta x_{R,a}} + \sum_{k \in \psi_{R,k}} (H_{k,r} A_{k,r} + H_{k,w} A_{k,w}) (\theta_{k,is} - \theta_{R,sur}) + h_{R,co} (A_{R,w} + A_{R,u}) (\theta_{R,uc} - \theta_{R,sur}) - q_{evp} A_{R,v} - q_{rad} A_{R,u} \quad \forall k \in \psi_{R,k}, R \in \psi_R. \quad (6)$$

where $\sum \rho_i c_i \Delta x_{R,i} A_{R,i}$ is the sum of the thermal mass of the wall and other surfaces; β_R is albedo in block R ; I_R is the solar radiation intensity; $k_{R,v}$ and $k_{R,a}$ are the conductivities of vegetated and man-made surfaces, respectively; $\theta_{R,wx,v}$ and $\theta_{R,wx,a}$ are the vegetated and man-made subsurface temperatures at effective depth Δx , respectively; $H_{k,r}$ and $H_{k,w}$ are the heat transfer coefficient of roof and wall of building k , respectively; q_{evp} and q_{rad} are the evapotranspiration heat flux and long-wave radiation heat flux to the sky, respectively. The remaining terms on the right-hand side represent solar insolation, the convective heat flux of vegetated and man-made ground surfaces, the convective heat flux of urban canopy layer air, the convective heat flux of building internal air, the evapotranspiration heat flux, and long-wave radiation heat flux to the sky.

airflow rate from urban boundary layer in block R , described in (2),^{42,43} $q_{k,is}$ is the ventilation rate from indoor of building k , described in (3); $E_{R,an}$ is the anthropogenic heat density in block R , which is calculated based on population density⁴⁴; $Q_{R,waste}$ is the total waste heat of air conditioner estimated to block R , described in (4); $h_{R,co}$ is the convective heat transfer coefficient between the external surface and the urban air in block R , described in (5).⁴⁵

The equation (1) shows the heat flux balance in the urban canopy layer. The remaining terms on the right-hand side represent the convective heat flux from the urban boundary layer, the waste heat flux of air conditioners, the convective heat flux from building indoors, the anthropogenic heat flux, and the convective heat flux from the external surface. The parameters calculation process is as follows:

$$q_{R,ubl} = [(L_R - x_{0,R}) L_R] (1 - \lambda_{p,R}) U_{E,R} \quad (2)$$

$$q_{is,R} = ACH_R \times A_{f,R} \times H_R \quad (3)$$

$$Q_{R,waste} = \sum_{k \in R} (1 + COP_k) P_{k,ac} \quad (4)$$

$$h_{R,co} = 5.7 + 3.8U_{E,R} \quad (5)$$

where L_R is the averaging length scale; $x_{0,R}$ is the length scale of order; $\lambda_{p,R}$ is building plan area density; $U_{E,R}$ is the mean wind speed; ACH_R is the air change time; $A_{f,R}$ is the lateral area of heat exchange between the control volume and its surroundings; H_R is the average building height; COP_k is the coefficient of performance of air conditioner of building k ; $P_{k,ac}$ is the electric power of air conditioner of building k .

The urban surface layer, which is an approximate calculation of the average temperature of all surfaces, includes the urban underlay, building walls, and roof surfaces. The control volume of the surface layer refers to the depth

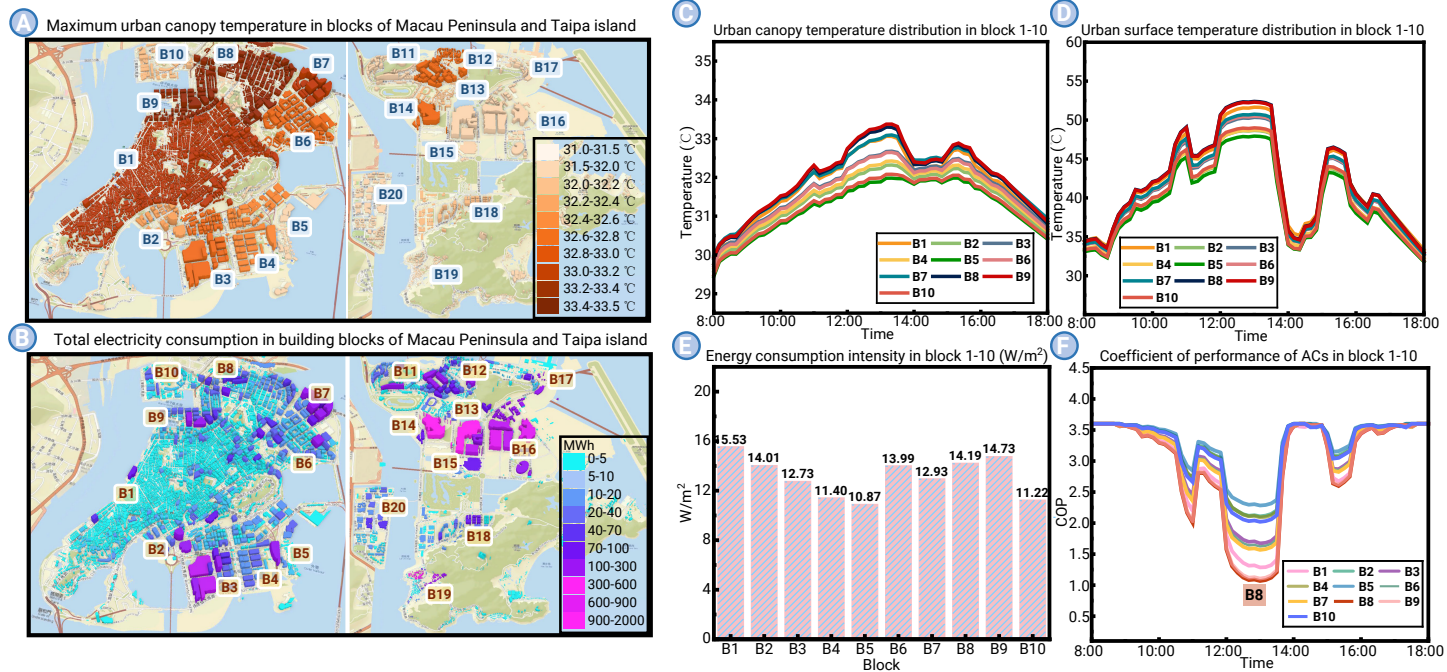


Figure 3. The vicious cycle impact in Macao.

in detail in Figure 1. We conducted tests on two different brands of air conditioners at various ambient temperatures to evaluate their performance. Based on the collected data, we derived an approximate numerical relationship between the coefficient of performance of the air conditioner and the ambient temperature, described in (8):

$$COP_{k,t} = \begin{cases} 3.6, & \text{if } \theta_{sur,t} \leq 35^\circ\text{C} \\ -0.01076_{sur,t}^2 + 0.7901\theta_{sur,t} - 11.0058, & \text{if } \theta_{sur,t} > 35^\circ\text{C} \end{cases} \quad (8)$$

The optimization model is proposed to arrange air conditioner operation schemes to achieve vicious cycle mitigation and energy saving. For each building block, the objective function is to minimize power consumption, as described in (9).

$$\min F_R = \sum_{t \in \psi_t} \sum_{k \in \psi_{R,k}} P_{k,ac,t} \Delta t \quad (9)$$

Besides, the optimization model needs to satisfy the above constraints in (1, 2, 3, 4, 5, 6, 7, 8), in addition to the operating capacity constraints of the air conditioner and the user's adjustable comfort constraints, described in (10, 11, 12):

$$P_{k,ac}^{\min} \leq P_{k,ac,t} \leq P_{k,ac}^{\max}, \forall k \in \psi_{R,k}, \forall t \in \psi_t \quad (10)$$

$$-DR_{k,ac} \leq P_{k,ac,t} - P_{k,ac,t-1} \leq UR_{k,ac}, \forall k \in \psi_{R,k}, \forall t \in \psi_t \quad (11)$$

$$\theta_{k,is}^{\min} \leq \theta_{k,is,t} \leq \theta_{k,is}^{\max}, \forall k \in \psi_{R,k}, \forall t \in \psi_t \quad (12)$$

where F_R is the objective function of block R ; Δt is the optimization time step; $P_{k,ac}^{\min}$ and $P_{k,ac}^{\max}$ are the minimum and maximum operating capacity constraints of air conditioners in building k , respectively; $DR_{k,ac}$ and $UR_{k,ac}$ are the down-ramp rate and up-ramp rate constraints of air conditioners in building k , respectively; $\theta_{k,is}^{\min}$ and $\theta_{k,is}^{\max}$ are the lower and upper indoor temperature of building k , respectively.

JOINT OPTIMIZATION MODEL DEMONSTRATION

Our joint model framework consists of an urban microclimate model and building system model, as presented in Figure 1. To numerically simulate the interaction of multi-type building clusters with their surrounding microclimate, we zone the urban underlying surface based on building density, building type, and vegetation cover in the horizontal direction. Moreover, the urban

vertical space is divided into urban boundary layer, urban canopy layer, and urban surface layer, as shown in Figure 1A. The temperature of the urban boundary layer is the data from geostationary operational environmental satellite, which is the initial condition and upper boundary of the canopy temperature. The urban canopy layer is a geographic space that directly affects human activity and health, while its shape is also influenced by building type. Sensible heat balance for the urban canopy layer includes the advection heat flux from the urban boundary layer, the convective heat flux from the external surface, the waste heat flux of the air conditioner, and the anthropogenic heat flux. Besides, sensible heat balance for the urban surface layer includes the solar insolation, the convective heat flux of vegetated and man-made ground surfaces, the convective heat flux of urban canopy layer air, the convective heat flux of building internal air, the evapotranspiration heat flux, and long-wave radiation heat flux to the sky.

The building energy model describes the heat flux balance inside a room, as shown in Figure 1B. The cooling generated by the air conditioner needs to offset convective heat flux from the roof surface and wall surface, the ventilated heat flux from air change, the transmission of solar insolation through the windows, the internal heat generation from the equipment and occupants. Simultaneously, the air conditioner is involved in energy system optimization in conjunction with the building's virtual energy storage. However, the air conditioner is merely an inefficient heat carrier, meaning that more waste heat needs to be generated and transferred outdoors to keep the room cool. In the summer, solar radiation heats the entire city through short-wave radiation. The rising urban canopy layer temperatures drive the use of air conditioners while generating large amounts of waste heat. Unfortunately, heat fluxes, including solar radiation, air conditioner waste heat, and anthropogenic heat, are accumulated within the high-density building stock due to building wind resistance and surface reflection. As time progresses and solar radiation intensifies, the heat accumulation in the limited space will push the urban canopy layer temperature to a spike.

Even worse, heat waves will damage the coefficient of performance (COP) of air conditioners. As in Figure 1C air condensing units are installed on the outer surface of the wall, resulting in its operating conditions being directly influenced by the urban surface layer. Inside the air conditioner, the refrigerant completes compression, evaporation, expansion, and condensation to achieve the transfer of heat flux between indoor and outdoor areas. Cycle 1-2-3-4-1 in Figure 1D depicts the physical states and energy changes of the refrigerant cooling process. For operating air conditioners, COP is related to evaporating temperature and condensing temperature. There is no signifi-

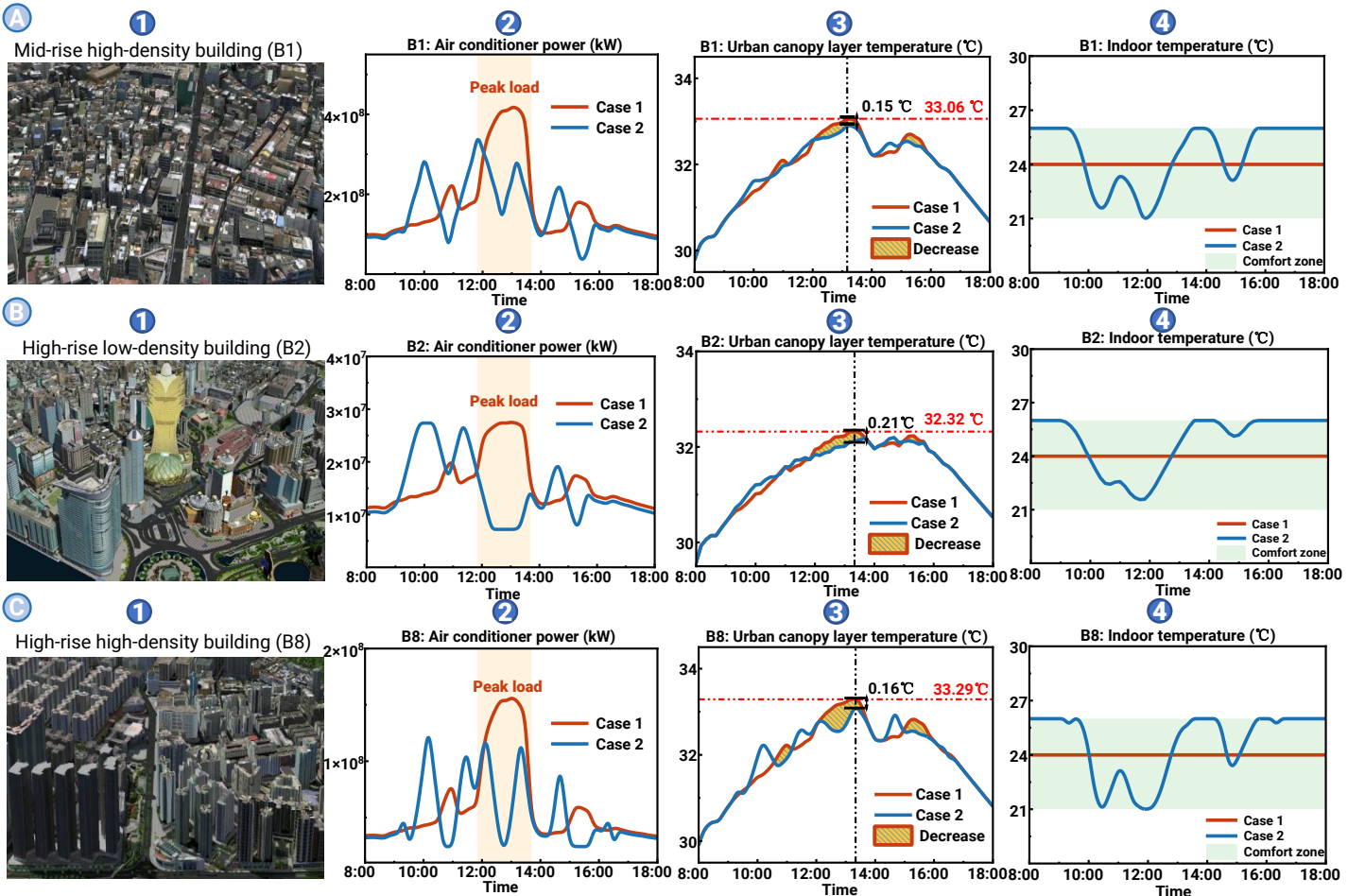


Figure 4. The optimization results in three typical building blocks (B1, B2, B8), in Macao.

can change in evaporative temperature as the room temperature is always kept within the comfort zone of the user. In contrast, the cooling air for the condenser tube originates from the surface of the wall, so the heat flux gathered at the surface layer will be fed into air condensing units, as in Figure 1E. When the temperature around the air condensing unit rises significantly, the refrigeration cycle will enter the process 1-2'-3'-4'-1. As can be seen from the pressure-enthalpy diagram, the compressor consumes more power with less cooling capacity accompanying the evaporation process, which undoubtedly exacerbates the decline in COP. To simulate the realistic operating conditions of air conditioners, we provide experimental data of two typical brands in the enthalpy difference chamber and fit the numerical relationship between ambient temperature and cooling capacity, as shown in Figure 1F. When the ambient temperature is less than 43°C, the air conditioner can maintain satisfactory efficiency. As the ambient temperature continues to rise, the energy efficiency of the air conditioner decreases rapidly as a quadratic function.

QUANTITATIVE ANALYSIS AND OPTIMAL DISPATCH IN MACAO

Macao is one of the most representative cities in the Greater Bay Area in terms of hot and humid meteorological conditions. In the past decade, the temperature in Macao has been rising continuously due to the influence of global warming Figure 2A. The hot climate leads to almost year-round cooling demand in Macao. Furthermore, the highest population density in the world (20,800 people/km²) and a thriving tertiary sector (92.3% of GDP in 2022) make it the most energy-intensive in the Greater Bay Area, with dense clusters of buildings being the largest energy-end. Based on the climatic characteristics and forms of energy use, the distribution of energy consumption in Macao is characterized by a clear seasonal and year-on-year growth (Figure 2B). Notably, in July, electricity consumption for building cooling already surpasses 60% of the total electricity consumption. The building GIS data of the Macau Peninsula and Taipa island are depicted in Figure 2C.

According to building density, height, and use type, we divide the buildings in the whole territory of Macao into 20 typical building blocks. For each block, the proposed model is implemented to quantitatively analyze and calculate the results of the interaction between microclimate and building energy systems. Further, we propose optimization strategies to mitigate the above vicious cycle.

The numerical analysis of the proposed vicious cycle in Macao is depicted in Figure 3, including the microclimate temperature distribution, building energy consumption, and cooling equipment efficiency. First, influenced by the vicious cycle, the maximum urban canopy temperatures in high-density building blocks, e.g., B1, B7, B8, and B9, are significantly higher than those in surrounding mid-density building blocks (Figure 3A). The main reason for this phenomenon is that high-density building blocks have higher wind resistance, more wall surfaces, and less green space, resulting in more anthropogenic waste heat and solar radiation heat accumulating in the canopy layer. Relative to the neighboring low-density building blocks, this temperature difference even exceeds 1.52°C in Macao. More seriously, under the same urban boundary layer conditions, high-density building blocks continue to experience rapid temperature increases during the midday period due to the vicious cycle (Figure 3C). This phenomenon reflects that during the midday period, the rise in temperature and solar radiation causes ACs to emit more waste heat, and the wind resistance in high-density building blocks prevents effective heat diffusion, exacerbating the temperature rise. Moreover, the temperature increase is more marked in the urban surface layer, owing to the much lower heat capacity. Comparing the high-density building block B9 with the low-density building block B5, the maximum temperature gap has reached 4.45°C (Figure 3D).

Second, the vicious cycle further exacerbates the cooling demand of individual buildings while raising the urban temperature. Figure 3B depicts the total electricity consumption in one day of cooling demand for the whole

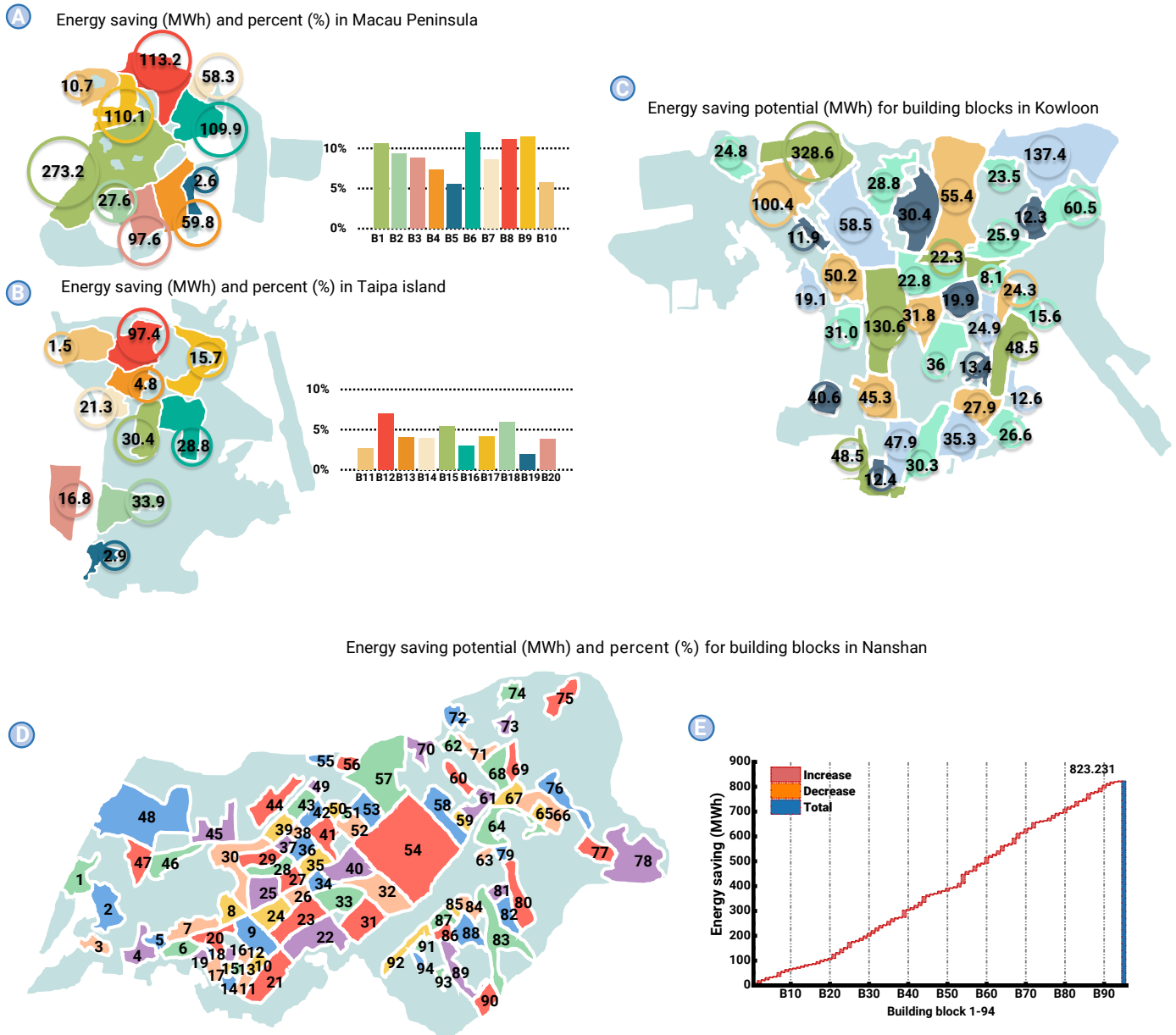


Figure 5. The energy saving potential for each building blocks.

territory of Macao. Based on the equation (7), it can be inferred that the electricity consumption of ACs is related to several key factors: ambient temperature (especially canopy and surface layer temperatures), solar radiation intensity, indoor anthropogenic heat density, and the structural parameters (especially building floors and area). Compared to residential buildings in B1, commercial buildings in B3, B4, B15, and B16, whose larger size and heat transfer area result in significantly higher total energy consumption. To further analyze the impact of the vicious cycle, 10 building blocks in the Macau Peninsula are chosen to calculate the cooling power consumption per unit area, which have the same boundary layer conditions and urban anthropogenic heat density (Figure 3E). Excluding the effect of building parameters, B1 consumes an additional 4.66 W/m² compared to the climate-friendly B5, representing an increase of 42.8%.

Third, the air conditioner is installed on the building surface, and its operating ambient temperature is approximated as the temperature of the urban surface layer. At midday, not only does wind resistance cause solar radiation to accumulate on the urban surface but also the temperature rise in the urban canopy reduces the rate of surface heat diffusion. As depicted in Figure 3D, the maximum temperature of the urban surface layer in the Macau Peninsula exceeds 45°C, even in the high-density blocks B1, B8, and B9,

where the temperature exceeds 50°C. Therefore, during periods of high solar radiation intensity and canopy temperatures, the COP of air conditioners will decrease as the temperature of the urban surface layer rises (Figure 3F). In B8, the COP reaches its lowest point, dropping briefly below 1.5, which is only 41% of its normal operation. Regrettably, periods of COP decline typically coincide with periods of increased demand for cooling in buildings, thereby amplifying electric peak loads and shocking the power supply system.

Mitigating the vicious cycle between urban microclimate and building energy systems is the key issue for energy saving and environment friendly. For most high-density building blocks, retrofitting buildings, expanding green space, and reducing population are costly or even difficult to achieve. Our joint optimization model supports urban thermal mitigation from the perspective of energy system operation. By exploiting virtual building energy storage and the user-adjustable comfort temperature, the optimized air conditioner operation scheme no longer follows the ambient temperature variation completely. We choose three typical building blocks to describe the details of the optimization process, containing mid-rise high-density B1, high-rise low-density B2, and high-rise high-density B8, as shown in Figure 4.

In case 1, the power demand curve for air conditioners is observed to follow the trend of urban canopy temperature to maintain a stable indoor

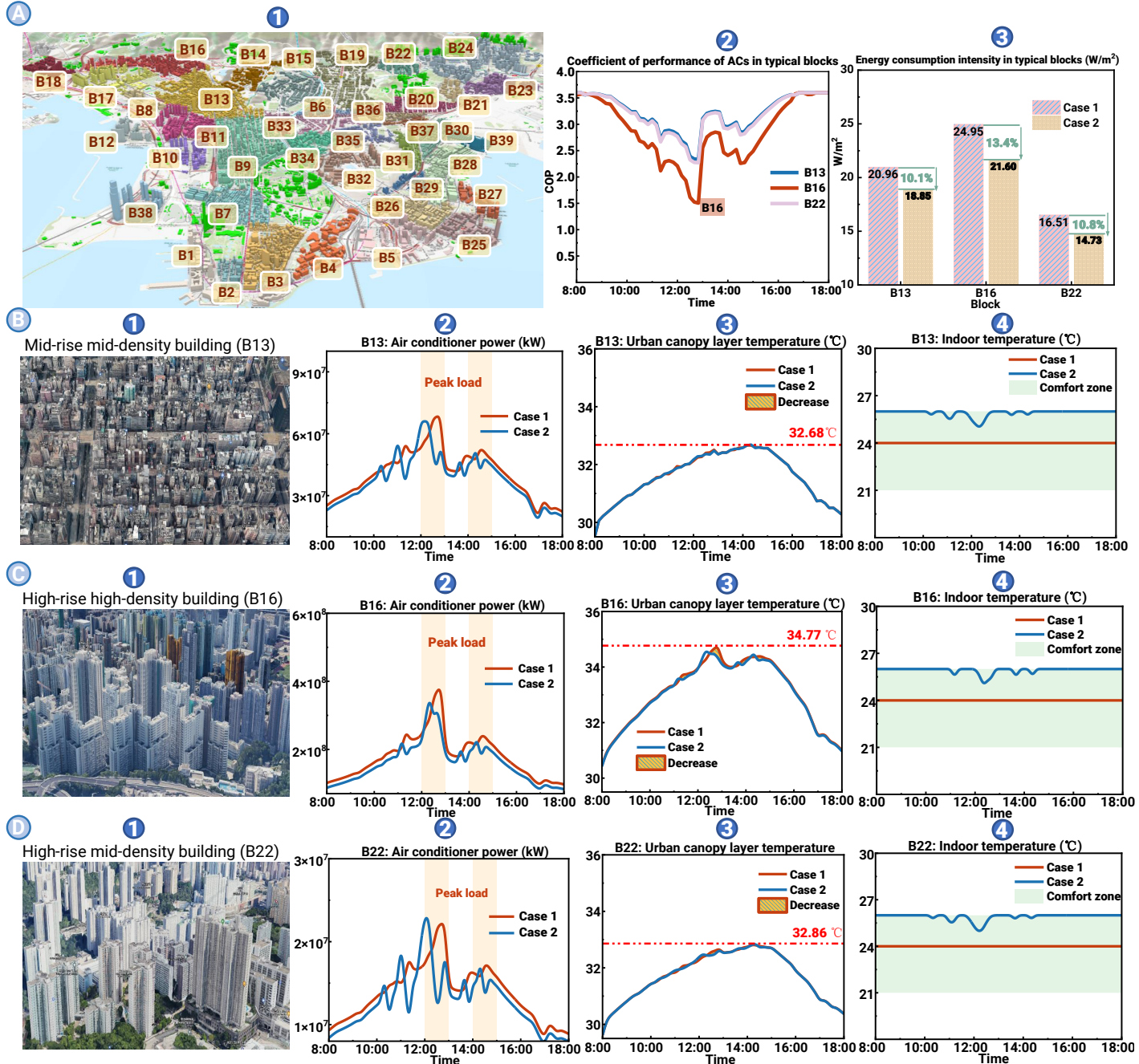


Figure 6. Buildings, COP and energy consumption characteristics of building blocks in Kowloon and the optimization result in three typical building blocks (B13, B16, B22).

temperature. At midday, the temperatures of the urban surface layer and canopy layer rise with the intensity of solar radiation, which directly leads to COP loss and higher electricity demand. In this dynamic interactive process, the continuous emission of waste heat from air conditioners will further aggravate the urban heat wave. During the period of 12:00–14:00, the peak power is already around three to five times greater than the valley, as depicted in Figure 4A-C column 2. Simultaneously, a large amount of waste heat is released into the building's surrounding air, resulting in a significant temperature rise. In particular, this vicious cycle is more severe in the high-rise high-density building blocks. According to Figure 4D, the COP of high-rise high-density B8 only reaches 52% of that in B2 at midday. By comparing the midday maximum temperatures in Figure 4 A-C column 3, we observe a temperature difference of 0.97°C between neighborhoods with high-density and low-density building blocks. Briefly, Case 1 illustrates that air conditioners have to sacrifice energy efficiency to meet cooling demand in the conventional operation mode, while continually exacerbating the urban heat waves.

In Case 2, we arrange the building pre-cooling based on the thermal inertia characteristics, which can provide an energy buffer to maintain the indoor temperature without a noticeable change (Figure 4 A-C column 4). Thus, the building's thermal inertia offers virtual energy storage to support load shifting of air conditioners during the conflicting periods of urban microclimate and building cooling demand. The blue line depicts two typical features of the air conditioner optimization results. On the one hand, building pre-cooling occurs before the COP drops to keep the air conditioner operating at a higher energy efficiency level. On the other hand, the peak loads of air conditioners are shifted before the higher urban temperatures come, ensuring that the waste heat is shifted and released in advance. In other words, we employ the proposed joint optimization model to break the vicious cycle from the energy system side and mitigate the extreme heat waves during the midday hours. For example, in Figure 4A(2) & (3), the peak-to-valley difference of the mid-rise high-density B1's electricity demand is effectively reduced, easing the maximum temperature of the urban canopy down by 0.15°C.

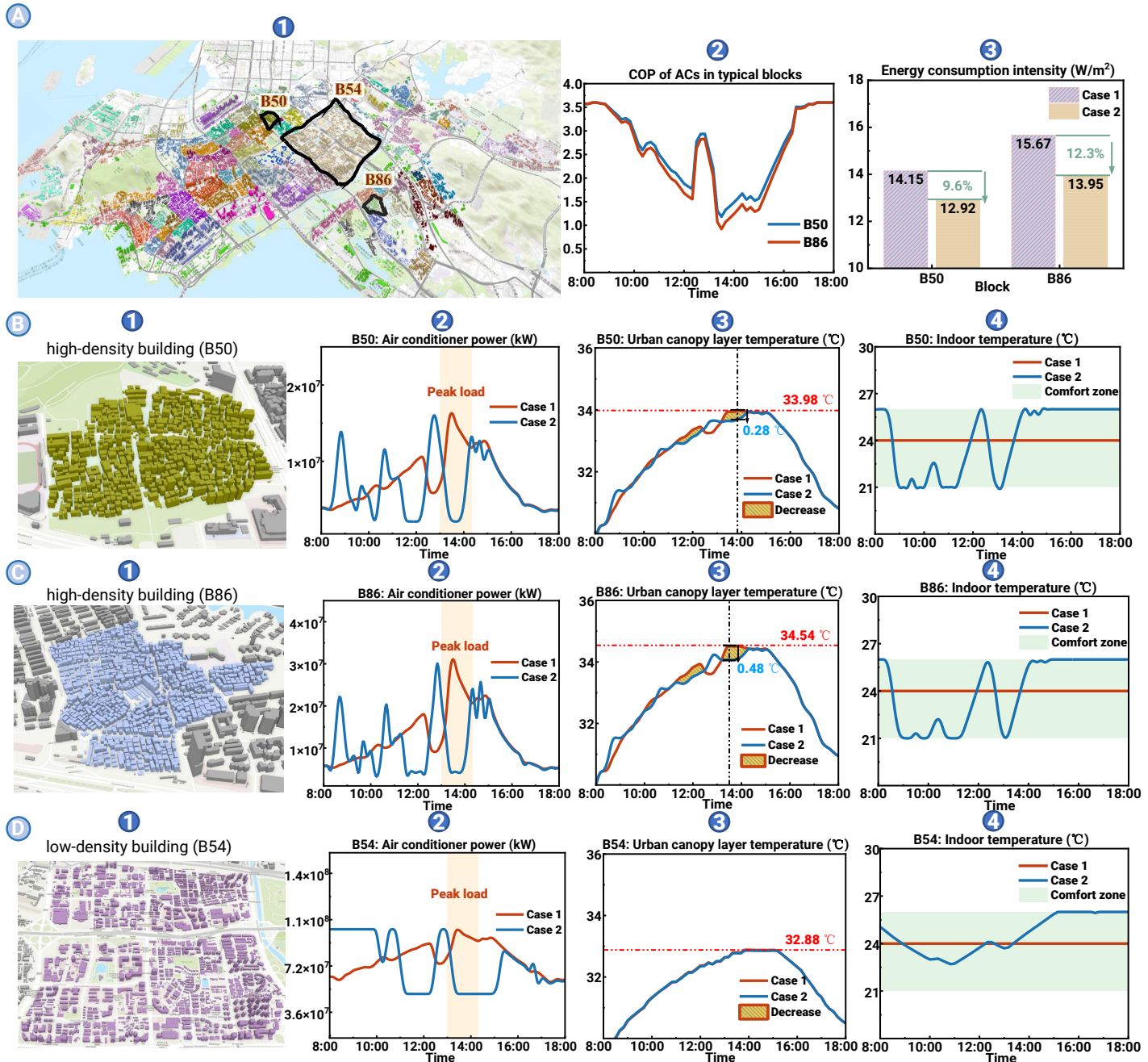


Figure 7. Buildings, COP and energy consumption characteristics of building blocks in Nanshan and the optimization result in three typical urban villages (B50, B86, B54).

The proposed model can effectively mitigate the vicious cycle between urban microclimate, building energy systems, and cooling equipment operation. The previous analysis of three typical blocks highlights that the optimal control of air conditioners can reduce urban overheating and energy consumption. The building energy saving volume and percent for Macao are presented in Figure 5A and Figure 5B. The optimization in a single day can save approximately 1116.5 MWh, which accounts for 8.2% of the total cooling electricity consumption in Macao. Notably, the energy-saving potential of each building block is associated with the building characteristics. It is evident that the high-density building blocks B1, B6, B8, and B9, which experience a more severe vicious cycle, exhibit a higher energy-saving potential of over 10%. Therefore, facing the challenges posed by global warming and advancing urbanization, building energy saving should not only focus on the energy side, but also devote greater attention to the interaction between building energy and surrounding microclimate conditions.

QUANTITATIVE ANALYSIS AND OPTIMAL DISPATCH IN KOWLOON, HONG KONG

Hong Kong, as the financial, transport, and trade center of the Greater Bay Area, owns one of the highest building densities worldwide. Particularly, the Kowloon area, which occupies a mere 47 km² (equivalent to 4.2% of Hong Kong's total land area), accommodates 30.1% of the city's population (2021). The population density of Kowloon is 44,926 people/km². The exploding population has resulted in the gradual proliferation of numerous high-rises and high-density buildings. Therefore, we select Kowloon as a representative case of Hong Kong. According to building density, height, and use type, we divide the buildings into 39 typical building blocks, as depicted in Figure 6A(1). For each block, the proposed model is implemented to quantitatively analyze and calculate the results of the interaction between microclimate and building energy systems.

Three typical building blocks are selected to give a detailed optimization analysis, including a mid-rise mid-density block (B13), a high-rise high-

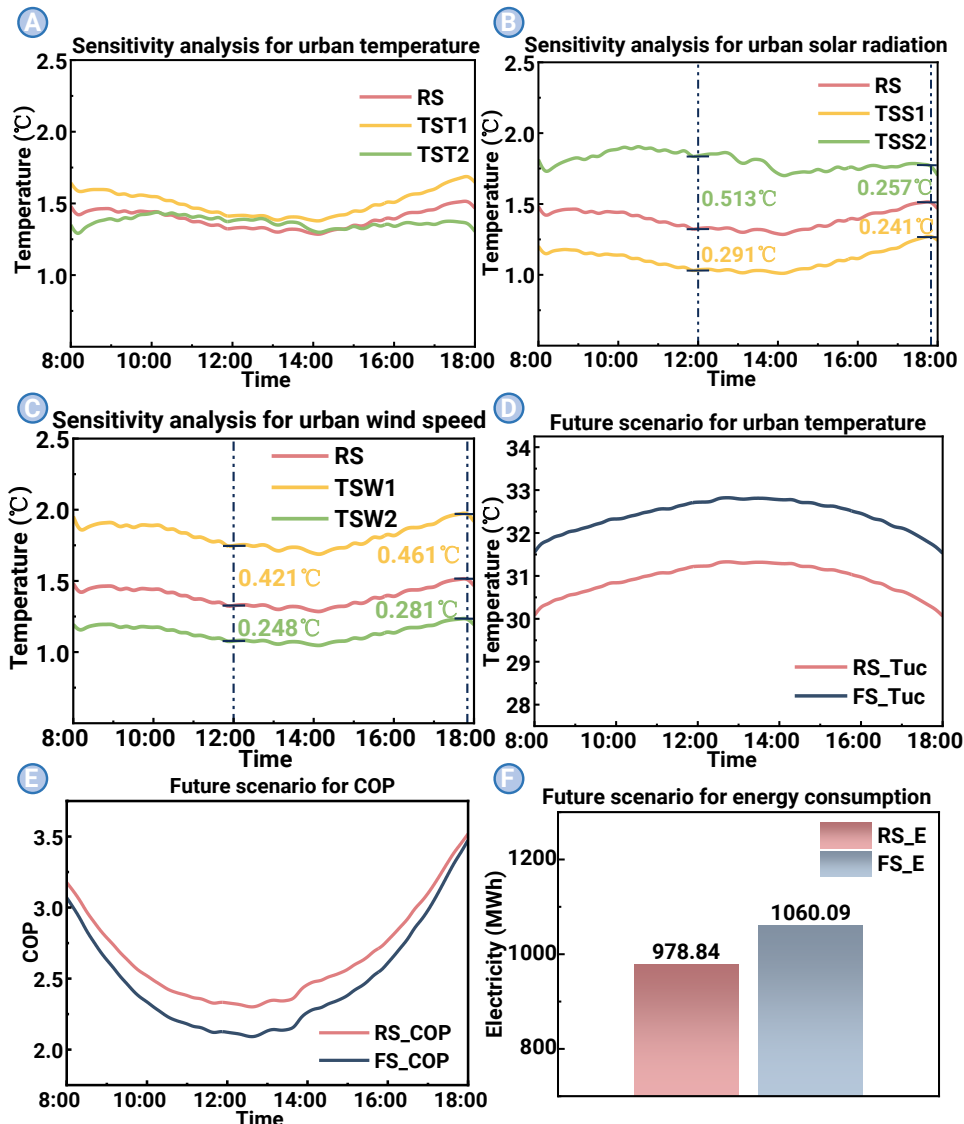


Figure 8. Sensitivity and future scenario analysis.

while maintaining a comfortable indoor temperature. On the one hand, increasing the air conditioner output and storing the cooling in the building during high COP phases can help reduce the additional power consumption caused by COP shrinkage. On the other hand, pre-cooling of the building enables the transfer of waste heat emissions and avoids exacerbating the vicious cycle during peak temperature hours. Hereby, the mitigation of the vicious cycle results in a 13.4% reduction in energy consumption density for the high-rise, high-density building block B16, as shown in Figure 6A(3). Additionally, Figure 5C illustrates the calculation of the energy saving potential of the entire Kowloon area, indicating that the joint model framework consists of urban microclimate model and building system model can achieve a one-day electricity saving of 1,724.71 MWh.

QUANTITATIVE ANALYSIS AND OPTIMAL DISPATCH IN NANSHAN, SHENZHEN

Shenzhen, the leading city in terms of GDP in the Greater Bay Area, has Nanshan District which achieved a GDP of over RMB 800 billion in 2022, ranking third among all districts and counties in China. Unlike Macau and Hong Kong, Nanshan District is characterized by numerous urban villages consisting of densely packed mid-rise buildings. Dense residential buildings will reduce natural ventilation, and the lack of greenery further exacerbates heat accumulation around the buildings, resulting in elevated urban canopy temperatures. Focusing on this issue, the buildings in Nanshan have been categorized into 94 blocks based on architectural characteristics, as depicted in

density block (B16), and a high-rise mid-density block (B22), as depicted in Figure 6. In the selected typical day, solar radiation and boundary layer temperature have two peak periods at 12:00-13:00 and 14:00-15:00. Case 1 illustrates the interaction among COP, electricity consumption of air conditioners, and canopy layer temperature in the vicious cycle. First, excessively high ambient temperatures result in heat dissipation efficiency reducing of air conditioner, meaning that the air conditioner consumes the same amount of electricity but produces less cooling capacity, as previously analyzed. This phenomenon is even more pronounced in the high-rise high-density block (B16) in Kowloon, as the COP drops even to 40% (Figure 6A(2)). Second, due to the combined effects of higher ambient temperature and COP loss, air conditioners have to increase operating power to maintain a constant indoor temperature. In three typical building blocks, it can be observed that the peak load of air conditioners is 2 to 3 times higher than the valley (Figure 6B-D column 2). Third, the air conditioner, as a heat porter, generates cooling capacity while emitting a significant amount of waste heat into the building surroundings. In the same boundary condition, the canopy temperature of the high-rise high-density block (B16) increases by 1.91°C compared to the high-rise mid-density building block (Figure 6B-D column 3). This is because the high-density building has greater wind resistance, allowing a significant accumulation of waste heat, solar heat, and anthropogenic heat inside the block. Eventually, under the vicious cycle, the energy density of B16 is increased by 51% compared to B22, as shown in Figure 6A(3).

By utilizing the proposed optimization model in case 2, air conditioners are arranged to pre-cool the building and release the building thermal inertia,

Figure 7A. Furthermore, three typical blocks have been selected for detailed analysis and optimization, comprising two high-density urban villages (B50, B86 shown in Figure 7B & C), and a contrasting low-density block (B54 shown in Figure 7D).

Urban villages consisting of dense mid-rise buildings (e.g., B50 and B86), exhibit the typical vicious cycle impact and greater optimization potential. In Case 1, before optimization, factors including building wind resistance, waste heat, anthropogenic heat, and the lack of green space contribute to elevated urban canopy temperatures. Compared to the low-density block B54, the maximum temperature in the urban villages B50 and B86 increased by 1.1°C and 1.66°C, respectively (Figure 7B(3) & C(3)). Meanwhile, the increase in urban temperature caused the COP loss in air conditioner operation. As depicted in Figure 7D, the COP is only 30% of the rated value during the midday hours. At this time, the power consumption of the air conditioner increases rapidly under the combined effect of the increase in urban temperature and the COP shrinkage. Especially at 13:00-14:30, when the vicious cycle intensifies, the maximum peak load even exceeds five times of the valley (Figure 7B(2) & C(2)). In addition, from Figure 7A(3), it can be observed that although almost all the urban villages are residential buildings, they still have high energy consumption density due to the vicious cycle.

Similar to Macau and Hong Kong, effective mitigation of the vicious cycle in urban villages can be achieved by applying the proposed optimization model in Case 2. It is worth noting that buildings in urban villages consist of mid-rise residential buildings with small thermal inertia. Therefore, to meet the requirements of transferring waste heat and indoor comfort, the air condi-

titioner power of urban villages B50 and B86 is adjusted more frequently, as shown in Figure 7B. Meanwhile, higher density block B86 demonstrates the effectiveness of the proposed model, achieving a reduction of the maximum temperature by 0.48°C (Figure 7C(3)) and a reduction of the energy consumption density by 12.3% (Figure 7A(3)).

Compared to urban villages with high-density buildings, B54, a low-density building block in Nanshan District, is less impacted by the vicious cycle. In Figure 7D, it can be noticed that in B54 the urban canopy temperature spikes are lower and the curve is smoother compared to the urban villages B50 and B86. Besides, comparing the air conditioner operating curves and indoor temperature changes in Case 1 and Case 2, it is illustrated that the virtual energy storage capacity of the building can support the air conditioner to maintain a low output level during the COP reduction period while meeting the comfort demand of the users. Finally, Figure 5D-E illustrates the calculation of the energy-saving potential of the entire Nanshan area, indicating that the proposed joint optimization model can achieve a one-day electricity saving of 823.231 MWh.

SENSITIVITY ANALYSIS

This paper focuses on the vicious circle between urban microclimate and building energy systems, for determining building blocks, its severity is directly influenced by city-scale meteorological conditions, particularly temperature, wind speed, and solar radiation. Here, the high-rise, high-density building block B8 on the Macau Peninsula is selected for sensitivity analysis. First, the meteorological parameters of the Macau Peninsula on a summer day in 2020 are selected as inputs for the reference scenario (RS). Then, the test scenarios are set up respectively based on the principle of variable uniqueness: the input temperature is adjusted downward by 25% as temperature test scenario 1 (TST1); the input temperature is adjusted upward by 25% as temperature test scenario 2 (TST2); the input solar radiation is adjusted downward by 25% as solar radiation test scenario 1 (TSS1); the input solar radiation is adjusted upward by 25% as solar radiation test scenario 2 (TSS2); the input wind speed is adjusted downward by 25% as wind speed test scenario 1 (TSW1); the input wind speed is adjusted upward by 25% as wind speed test scenario 2 (TSW2). The contribution of the vicious cycle to the urban canopy temperature increases under the different test scenarios described above is depicted in Figure 8A-C.

When comparing temperature increases across different test scenarios, it is clear that the vicious cycle is most sensitive to solar radiation. As depicted in Figure 8B, the temperature difference caused by equal-amplitude solar radiation adjustments reaches 0.513°C during midday hours. Compared to other parameters, the primary factor in the exacerbation of the vicious cycle by excessively high solar radiation intensity is twofold: First, solar radiation severely increases the temperature of the urban surface layer in building blocks with extensive man-made surfaces. The constant absorption of heat by building walls not only heats the urban air but also reduces the energy efficiency of air conditioners. Second, solar radiation heating indoor temperatures through windows causes higher indoor cooling demand, which in turn emits more waste heat into the surrounding environment. In contrast to solar radiation, the effects of urban temperature and urban wind speed exhibit consistent intra-day characteristics. Smaller effects are observed during the hot midday hours, while larger effects are seen during the cooler morning and evening hours. Notably, the impact of wind speed changes is more pronounced. At 18:00, a 25% decrease in wind speed will result in an additional 0.461°C temperature increase compared to the reference scenario. Especially in high-density building blocks, a reduction in urban-scale wind speed further exacerbates the accumulation of anthropogenic heat around buildings.

The above analysis discusses the impact of the current vicious cycle between urban microclimate and building energy systems on the Guangdong-Hong Kong-Macao Greater Bay Area. Furthermore, as depicted in Figure 2, the average temperature in Macao during July has increased by 1°C over the past decade. Given the intensification of global warming, it is crucial to account for the risks of climate change in the coming decade scenario. Based on the IPCC predictions and Macao's temperature trends, we set the future scenario (FS) to reflect a 1.5°C increase compared to the reference scenario (RS). Simulation results for high-rise and high-density building blocks in

Macao are presented in Figure 8D-F. The data shows that the vicious cycle between building neighborhoods and rising temperatures intensifies as the city's temperature increases. In the future scenario, the urban canopy temperature rises uniformly, as depicted in Figure 8D. This temperature increase also affects the urban surface layer, which directly interacts with the canopy layer, further deteriorating the operating conditions of air-conditioning condensing units. As a result, the operational efficiency of air conditioners will decline more severely in future scenarios, particularly during midday hours. Additionally, the temperature rise leads to higher building cooling demands, while the reduced operating efficiency of air conditioning systems exacerbates energy consumption. As can be seen in Figure 8F, the building energy consumption rises by 8.3% under the influence of the vicious cycle when the temperature of the future scenario increases by 1.5°C .

DISCUSSION

Urban heatwaves have swept through major cities around the world, and human activities are still increasingly exacerbating the risk of extreme urban microclimate. Particularly in the building energy sector, a vicious cycle between growing cooling demand and urban heat waves has become evident. In this study, an optimization model coupled with an urban microclimate model, a building energy system model, and a cooling equipment efficiency model are proposed to quantitatively describe the consequences of this vicious cycle. And, the proposed mitigation strategies are validated in the Guangdong-Hong Kong-Macao Greater Bay Area, which has typical high temperature and high humidity climatic conditions.

Our study points out that the vicious cycle between urban heatwaves and building energy systems is already widespread in dense building blocks. In cases of Guangdong-Hong Kong-Macao Greater Bay Area, waste heat emitted from building energy systems tends to accumulate in urban neighborhoods, leading to a temperature difference of $0.97\text{--}1.91^{\circ}\text{C}$ between high-density and low-density building blocks. This temperature rise directly impairs the efficiency of cooling equipment, resulting in only 30% to 52% of its rated value during peak heatwaves. Consequently, the building energy system has to consume more electricity to maintain a cool room, under the double pressure of temperature rise and COP drop. The resulting peak loads are 3 to 5 times higher than the valley and the average energy consumption increases by 42.8% to 51%.

We provide a paradigm for addressing global urban heat waves from a building energy perspective. Our proposed model demonstrates that the utilization of virtual energy storage in buildings can effectively mitigate the vicious cycle without retrofitting existing buildings. By rationalizing building pre-cooling before urban temperature rises and COP drops, it prevents to emitting of significant amounts of waste heat, which would otherwise exacerbate urban heatwaves and increase energy consumption. The proposed optimization strategy supports typical building blocks in the Guangdong-Hong Kong-Macao Greater Bay Area to reduce the urban heatwaves by 0.48°C , reduce the average energy density by 13.4%, and effectively shift the peak loads.

Our findings indicate a novel direction in the field of building energy system optimization, specifically focusing on the interactions with urban microclimate. Through the Guangdong-Hong Kong-Macao Greater Bay Area cases, our optimization model shows significant effectiveness in high-density commercial buildings, high-rise high-density office buildings, and high-density urban villages. By implementing the proposed strategy, the energy-saving potential of building blocks can reach 11.2%, 13.4%, and 12.3%, and save 1116.5 MWh, 1724.71 MWh, and 823.23 MWh in the three typical areas, respectively.

Persistent global warming and urbanization are exposing cities to increased climate risks, health crises, and energy shortages. Interdisciplinary urban research, covering urban weather, energy systems, and building sectors, has become more urgent than ever. On the one hand, the planning, construction, operation, and management of energy and building systems need to consider the impact on urban microclimate. Renewable energy, new materials, intelligent and refined management technologies, advanced prediction and control technologies, and efficient energy conversion and utilization technologies are essential for achieving sustainable, green, and healthy urban development. On the other hand, urban policymakers need to

establish interdisciplinary communication platforms and big data fusion and sharing systems to prompt interdisciplinary research. Additionally, market regulations and policy incentives are crucial to encourage active participation in urban governance.

REFERENCES

- Birkel S. (2023). Daily 2-meter Air Temperature, Climate Change Institute. Preprint at <https://ClimateReanalyzer.org>.
- European Centre for Medium-Range Weather Forecasts. (2023). European heatwave July 2023. Preprint at <https://www.ecmwf.int/>.
- Network. C. M. D. (2023). Ground-based observations in China. Preprint at <https://data.cma.cn/>.
- Patz J. A., Campbell-Lendrum D., Holloway T., et al. (2005). Impact of regional climate change on human health. *Nature* **438**:310–317. DOI:10.1038/nature04188
- IEA. (2018). The Future of Cooling. Preprint at <https://www.iea.org/reports/the-future-of-cooling>.
- IEA. (2018). Share of cooling in electricity system peak loads in selected countries/region, baseline and cooling scenario. Preprint at <https://www.iea.org/data-and-statistics/charts>.
- Song M., Deng R., Yan X., et al. (2024). Two-stage decision-dependent demand response driven by TCLs for distribution system resilience enhancement. *Appl. Energy* **361**:122894. DOI:10.1016/j.apenergy.2024.122894
- Qi T., Ye C., Hui H., et al. (2024). Fast Frequency Regulation Utilizing Non-Aggregate Thermostatically Controlled Loads Based on Edge Intelligent Terminals. *IEEE Trans. Smart Grid* **15**:3571–3584. DOI:10.1109/TSG.2023.3346467
- Chen G., Zhang H., Hui H., et al. (2021). Fast Wasserstein-Distance-Based Distributionally Robust Chance-Constrained Power Dispatch for Multi-Zone HVAC Systems. *IEEE Trans. Smart Grid* **12**:4016–4028. DOI:10.1109/TSG.2021.3076237
- Yu P., Zhang H., Song Y., et al. (2024). District Cooling System Control for Providing Operating Reserve Based on Safe Deep Reinforcement Learning. *IEEE Trans. Power Sys.* **39**:40–52. DOI:10.1109/TPWRS.2023.3237888
- Chen L. and Hui H. (2025). Model Predictive Control-Based Active/Reactive Power Regulation of Inverter Air Conditioners for Improving Voltage Quality of Distribution Systems. *IEEE Trans. Ind. Inf.* **21**:922–931. DOI:10.1109/TII.2024.3468475
- Liu R., Hui H., Chen X., et al. (2024). Distributed Frequency Control of Heterogeneous Energy Storage Systems Considering Short-Term Ability and Long-Term Flexibility. *IEEE Trans. Smart Grid* **15**:5693–5705. DOI:10.1109/TSG.2024.3451614
- Zhang Z., Hui H. and Song Y. (2025). Response Capacity Allocation of Air Conditioners for Peak-Valley Regulation Considering Interaction with Surrounding Microclimate. *IEEE Trans. Smart Grid* **16**:1155–1167. DOI:10.1109/TSG.2024.3482361
- Rizwan A. M., Dennis L. Y. and Chunho L. (2008). A review on the generation, determination and mitigation of Urban Heat Island. *J. Environ. Sci.* **20**:120–128. DOI:10.1016/S1001-0742(08)60019-4
- Grimm N. B., Faeth S. H., Golubiewski N. E., et al. (2008). Global change and the ecology of cities. *Science* **319**:756–760. DOI:10.1126/science.1150195
- Rajagopalan P., Lim K. C. and Jamei E. (2014). Urban heat island and wind flow characteristics of a tropical city. *Solar Energy* **107**:159–170. DOI:10.1016/j.solener.2014.05.042
- Zhao L., Lee X., Smith R. B., et al. (2014). Strong contributions of local back-ground climate to urban heat islands. *Nature* **511**:216–219. DOI:10.1038/nature13462
- Cao C., Lee X., Liu S., et al. (2016). Urban heat islands in China enhanced by haze pollution. *Nat. Commun.* **7**:12509. DOI:10.1038/ncomms12509
- Sun Y., Zhang X., Ren G., et al. (2016). Contribution of urbanization to warming in China. *Nat. Clim. Change* **6**:706–709. DOI:10.1038/nclimate2956. DOI:10.1038/nclimate2956
- Song Y., Zhang Z. and Hui H. (2024). Interdisciplinary collaborative perspectives: Urban microclimate, urban energy systems, and urban building sectors. *Innov. Energy* **1**:100053. DOI:10.59717/j.xinn-energy.2024.100053
- Tremeac B., Bousquet P., Munck C. de, et al. (2012). Influence of air conditioning management on heat island in Paris air street temperatures. *Appl. Energy* **95**:102–110. DOI:10.1016/j.apenergy.2012.02.015
- Santamouris M., Paolini R., Haddad S., et al. (2020). Heat mitigation technologies can improve sustainability in cities. An holistic experimental and numerical impact assessment of urban overheating and related heat mitigation strategies on energy consumption, indoor comfort, vulnerability and heat-related mortality and morbidity in cities. *Energy Build.* **217**:110002. DOI:10.1016/j.enbuild.2020.110002.
- Santamouris M. (2020). Recent progress on urban overheating and heat island research. *Integrated assessment of the energy, environmental, vulnerability and health impact. Synergies with the global climate change. Energy Build.* **207**:109482. DOI:10.1016/j.enbuild.2019.109482
- Craig M. T., Wohland J., Stoop L. P., et al. (2022). Overcoming the disconnect between energy system and climate modeling. *Joule* **6**:1405–1417. DOI:10.1016/j.joule.2022.05.010
- Haddad S., Paolini R., Ulpiani G., et al. (2020). Holistic approach to assess co-benefits of local climate mitigation in a hot humid region of Australia. *Sci. Rep.* **10**:14216. DOI:10.1038/s41598-020-71148-x
- Central C. (2021). Hot Zones: Urban Heat Islands. Preprint at <https://www.climatecentral.org/report/hot-zones-urban-heat-islands>.
- Javanroodi K., Nik V. M., Giometto M. G., et al. (2022). Combining computational fluid dynamics and neural networks to characterize microclimate extremes: Learning the complex interactions between meso-climate and urban morphology. *Sci. Total Environ.* **829**:154223. DOI:10.1016/j.scitotenv.2022.154223
- Salamanca F., Georgescu M., Mahalov A., et al. (2014). Anthropogenic heating of the urban environment due to air conditioning. *J. Geophys. Res. A* **119**:5949–5965. DOI:10.1002/2013JD021225
- Salamanca F., Martilli A. and Yagüe C. (2012). A numerical study of the Urban Heat Island over Madrid during the DESIREX (2008) campaign with WRF and an evaluation of simple mitigation strategies. *Int. J. Climat.* **32**:2372–2386. DOI:10.1002/joc.3398
- Wen Y. and Lian Z. (2009). Influence of air conditioners utilization on urban thermal environment. *Appl. Therm. Eng.* **29**:670–675. DOI:10.1016/j.aplthermaleng.2008.03.039
- Krøp A. (2009). Development and application of a numerical simulation system to evaluate the impact of anthropogenic heat fluxes on urban boundary layer climate. Ph.D thesis. Swiss Federal Institute of Technology Lausanne.
- Kikegawa Y., Genchi Y., Yoshikado H., et al. (2003). Development of a numerical simulation system toward comprehensive assessments of urban warming countermeasures including their impacts upon the urban buildings' energy-demands. *Appl. Energy* **76**:449–466. DOI:10.1016/S0306-2619(03)00009-6
- Kikegawa Y., Genchi Y., Kondo H., et al. (2006). Impacts of city-block-scale countermeasures against urban heat-island phenomena upon a building's energy-consumption for air-conditioning. *Appl. Energy* **83**:649–668. DOI:10.1016/j.apenergy.2005.06.001
- Bueno B., Norford L., Hidalgo J., et al. (2013). The urban weather generator. *J. Build. Perform. Sim.* **6**:269–281. DOI:10.1080/19401493.2012.718797
- Bueno B., Hidalgo J., Pigeon G., et al. (2013). Calculation of air temperatures above the urban canopy layer from measurements at a rural operational weather station. *J. Appl. Meteor. Climat.* **52**:472–483. DOI:10.1175/JAMC-D-12-083.1
- Ohashi Y., Genchi Y., Kondo H., et al. (2007). Influence of air-conditioning waste heat on air temperature in Tokyo during summer: Numerical experiments using an urban canopy model coupled with a building energy model. *J. Appl. Meteor. Climat.* **46**:66–81. DOI:10.1175/JAM2441.1
- Santamouris M. (2014). On the energy impact of urban heat island and global warming on buildings. *Energy Build.* **82**:100–113. DOI:10.1016/j.enbuild.2014.07.022
- Li X., Sun B., Sui C., et al. (2020). Integration of daytime radiative cooling and solar heating for year-round energy saving in buildings. *Nat. Commun.* **11**:6101. DOI:10.1038/s41467-020-19790-x
- Centre N. W. S. D. (n.d.). Preprint at <http://data.cma.cn/>.
- Geographic Sciences I. of and Natural Resources Research C. (n.d.). Resource and Environment Science and Data Center. Preprint at <https://www.resdc.cn/data.aspx?DATAID=270>.
- OpenStreetMap (n.d.). Preprint at <https://www.openstreetmap.org/>.
- Duan S., Luo Z., Yang X., et al. (2019). The impact of building operations on urban heat/cool islands under urban densification: A comparison between naturally-ventilated and air-conditioned buildings. *Appl. Energy* **235**:129–138. DOI:10.1016/j.apenergy.2018.10.108
- Coccol O. and Belcher S. (2005). Mean winds through an inhomogeneous urban canopy. *Bound. Meteor.* **115**:47–68. DOI:10.1007/s10546-004-1591-4
- Sailor D. J., Georgescu M., Milne J. M., et al. (2015). Development of a national anthropogenic heating database with an extrapolation for international cities. *Atmos. Environ.* **118**:7–18. DOI:10.1016/j.atmosenv.2015.07.016
- McAdams W. H. (1954). *Heat transmission* (3rd ed.). (New York: McGrawHill).

FUNDING AND ACKNOWLEDGMENTS

This work is funded in part by the National Natural Science Foundation of China (Grant no. 52407075), in part by the Science and Technology Development Fund, Macau SAR (File no. 001/2024/SKL and File no. 0117/2022/A3), and in part by the Chair Professor Research Grant of University of Macau (File no. CPG2025-00023-IOTSC).

AUTHOR CONTRIBUTIONS

ZZ.W. contributed to the conceptualization, data curation, software, formal analysis, investigation, visualization, methodology, and writing. HX.H. contributed to the conceptualization, data curation, software, methodology, and writing. YH.S. contributed to the conceptualization, resources, supervision, funding acquisition, and project administration.

DECLARATION OF INTERESTS

Professor Yonghua Song is an Editorial Board member of The Innovation Energy and was blinded from reviewing or making final decisions on the manuscript. Peer review was handled independently of this member and their research group. The other authors declare no conflicts of interest.

DATA AND MATERIALS AVAILABILITY

All data and materials are available from the corresponding author on request.